

**R. MERWINSKI and L. GUDZOWSKA**

*Ukrainian Academy of Printing, Lviv, Pidvalna 9 a, Lviv, Ukraine*

## **TiC Nanocrystals Embedded in Oligoetheracrylate Photopolymer Matrices as New Promising Nonlinear Optical Materials**

### **1. Introduction**

One can recently observe increasing interest in semiconductor nanocrystals due to a possibility of operation by the optical coefficients using size-dependent electron and optical properties [1–5]. Especial interest is connected to the semiconductor nanocrystals because the theoretical calculations [6,7] predict possibility of enhancement the nonlinear optical susceptibilities in the such type of the nanocrystallites.

However for a wide application of the nanocrystallites in optoelectronics there appears to be a complication because it is a necessity of preparation of high-quality homogeneous specimens. Usually the specimens are prepared like a film deposited on the dielectric subtract. In this case a main problem appears to be a high light scattering background. To eliminate this problem one can suggest the guest-host polymer technique [8 – 10] to the powder-like nanocrystallies. Such technique has been used in the Ref. 11 for  $\text{Sn}_2\text{P}_2\text{S}_6$  semiconductor nanocrystallites embedded in the oligoetheracrylate photopolymer matrices. It was shown that better technological parameters (lower light scattering losses, optical homogeneity, higher transparency etc) are achieved when the external electric field favors orientation of the embedded powder-like nanocrystallites. Another important reserve for enhancement of the nonlinear optical susceptibilities consists in additional photoexciting of the chromophores (in our case nanocrystallites) to enhance the appropriate matrix dipole momenta determining the output nonlinear optical susceptibilities [12].



Among the semiconducting nanocrystallites the TiC have been chosen because for these materials technology of preparation the specimens with desired sizes have been good approved for the SiC [13,14]. At the same time theoretical simulation predict [15] possibility of the large second-order nonlinear optical effects. The calculated electron charge density distributions in the oligoetheracrylate photopolymers [16 – 18] indicate on a good complementation of the polymers to the binary semiconductors because the appropriate matrix dipole moments are collinear. Another important advantageous of the oligoetheracrylate matrices consists in good mechanical and acoustooptical properties [19] determining the photoinduced response in the investigated materials.

In the present paper we will present the experimental results of the photoinduced nonlinear optical phenomena in the TiC nanocrystallites embedded in the oligoetheracrylate photopolymer matrices. In the Section 2 technology of specimen preparation and measurement setup is presented. Sec. 3 is devoted to the study of the photoinduced SHG versus temperature and photoinducing flux. Appropriate discussion of the obtained results as well the possible application are discussed.

## 2. Experimental details

### 2.1. Sample preparation

The TiC nanopowders were synthesized by a CO<sub>2</sub> laser pyrolysis from a gaseous mixture of TiH<sub>4</sub> and C<sub>2</sub>H<sub>2</sub> following the technology procedure described elsewhere [14]. Annealing of these powders has been performed under argon during one hour in a high temperature graphite furnace. Structural modifications, coalescence of the TiC grains and a removal of free carbon are induced by these heat treatment.

A crucial annealing temperature within the 1200 - 1700°C induces drastic changes on the TiC structures, the grain morphology and on the network composition. Varying the crucial annealing temperature continuously we change the nanometer sizes. The scanning electron microscopy (SEM) microscopy have been used for size definition of the nanopowder specimens.

All the powder-like specimens were embedded within the liquid oligoetheracrylate photocomposition [16-18] and were solidified using the nitrogen laser of the 45 W/cm<sup>2</sup> power and electropoling procedure described in the Ref. 11. The optimal electric field was equal to 400 V/cm and concentration corresponds to 0.21 % in weighting percent. Using the X-ray diffractometry a parameter of hexagonality *H* have been introduced. The latter have been determined as a ratio of hexagonal to cubic structural components in the mentioned TiC nanocrystallites. The latter are closely connected with the nanocrystallite sizes (see Table 1).



**Table 1. Structural parameters of the investigated TiC data: d- sizes of the particular nanoparticles (in nm); L — sizes of the grains (in nm); H — degree of hexagonality. In the brackets are given the parameters of the averaged dispersion the sizes**

Specimen	D [nm]	L [nm]	H
1	13.2 (0.2)	32 (0.2)	0.04
2	14.4 (0.2)	57 (0.2)	0.22 (0.2)
3	16.8 (0.2)	66 (0.2)	0.35 (0.2)
4	19.1 (0.2)	56 (0.2)	0.61 (0.2)
5	22 (0.2)	38 (0.2)	0.77 (0.2)
6	26 (0.2)	32 (0.2)	0.92 (0.2)

The X-ray monitoring were carried out using a DRON-2.0 diffractometer equipped with a horizontal goniometer GUR-5. The applied X-ray diffraction measurements had a molybdenum target ( $\lambda_{K\alpha} = 0.7169 \times 10^{-10}$  m) and a graphite monochromator in the primary beam. The surfaces of the specimens before the measurements were etched by the 7% weight water solution.

## 2.2. Nonlinear optical setup

Photoinducing light beams have been generated by Q-switched nitrogen laser ( $\lambda = 337$  nm) (light power about 25 MW with a pulse width varying within the 400 – 980 ps) (see Fig. 1). Quartz beam-splitter (BS1, BS2) form the photoinducing and probing laser beams. The value of pulse duration was defined by condition of avoiding specimen overheating. Rotating Fresnel prisms have been supplied by special equipment in order to operate by incident light polarization. The incident angle has been defined within the 2 – 24 degree. The maximal scattering optical background was less than 0.01%. Such wide ranges of the angle variation have been requested by necessity to achieve maximal output PISHG signal. We will show below that phase synchronism conditions play in this case central role. The diameter of the light beam spot is varied within the 16 – 1240  $\mu$ m and depending on the surface quality we vary the light spot diameter to achieve the maximal output PISHG signal. Moreover the setup allows scanning by the beam through the surface of specimen.

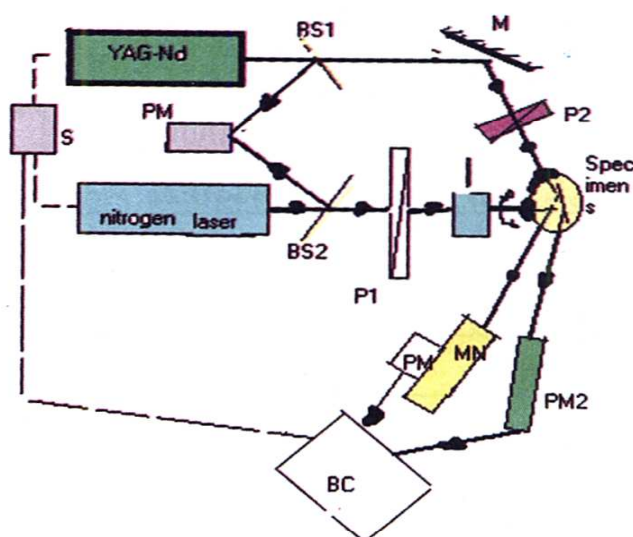


**Fig. 1.** Experimental setup for performing the photoinducing nonlinear optical measurements

The sequence of the beam has the gaussian-like shape with the dispersion half-width about 78%. Stability of the laser generation was not worse than 0.17%. The generation of the photoinducing nitrogen laser was synchronized in time with the generation of the probing YAG:Nd laser. We use unfocused YAG:Nd ( $\lambda = 1.06 \mu\text{m}$ ) laser beam (spot diameter 0.2 ... 13.6 mm; laser power 6 ... 14 MW; pulse duration 1.3 ... 1850 ps). Time repetition of the pulses was synchronized in time for the photoinducing and probing laser beams up to 0.2 ps. For the polarization of the photoinducing and probing beams. We use Glan-Thompson polarizers (P1,P2) with degree of polarizability about 99.998(7)% in the considered spectral range have been used. Electrooptically operated delaying line (I) on the ground of the  $\text{Li}_2\text{B}_4\text{O}_7$  single crystals has been applied for operation by the pump-probe time delay. This allows to vary the delaying time with resolution not worse than 0.6 ps. For the justification of the laser beams the lasers were supplied additionally with low power He-Ne lasers for hitting of the beams on the specimen surface. As a consequence any misbalance between the laser beams will be corrected. For the every specimens the measurements are done in more than 95 points to achieve reliable statistical averaging within the  $\chi^2$  Student distribution not worse than 0.02.

Photodetection has been carried out by digital high-resolution multipliers RCA-121 and FE-124-H (PM1, PM2) connected with boxcar (BC) with the gate about 480 ps. The grating monochromator (MN) SPM-3 (spectral resolution 7 nm/mm) have been used to separate green doubled frequency signal ( $\lambda = 0.53 \mu\text{m}$ ) from the YAG:Nd laser ( $\lambda = 1.06 \mu\text{m}$ ) background. Independ-



ently both pumping and probing signals were controlled by the connected synchronized photomultipliers (PM).

### 3. Experimental results and discussion

The measured dependences of the photoinduced SHG intensity as a function of the photoinducing nitrogen laser pump flux  $I$  and hexagonality  $H$  have been done (see Fig. 2). With increasing power of the photoinducing nitrogen laser pulses the SHG maximum output signal increases and achieves its maximum at the pumping photon fluxes about  $1.6 \text{ GW/cm}^2$ . It is necessary to underline that the maximum photoinduced SHG is achieved for the hexagonality about 0.95 and is equal about  $10.1 \pm 0.13 \text{ pm/V}$ . The measurements have been carried out for different concentration of the nanocrystallite chromophores. The investigations have shown that the optimal concentration of the embedded TiC nanopowders lies within the 0.8 – 1.6%. The maximal output SHG signal has been achieved for delaying time between photoinducing and probing beam about 20 ps. The main output SHG is observed for the  $\chi_{222}$  tensor components (where axis 2 is parallel to UV-photoinducing laser polarisation and applied electropoling field). All the presented data are obtained for temperature range within the 4.2 – 20 K because for the higher re-orientation temperature destroying long-range ordering is observed. Phase matching synchronism conditions are satisfied within the angle ranges  $4 - 11^\circ$ . All the presented data are averaged over the presented materials.

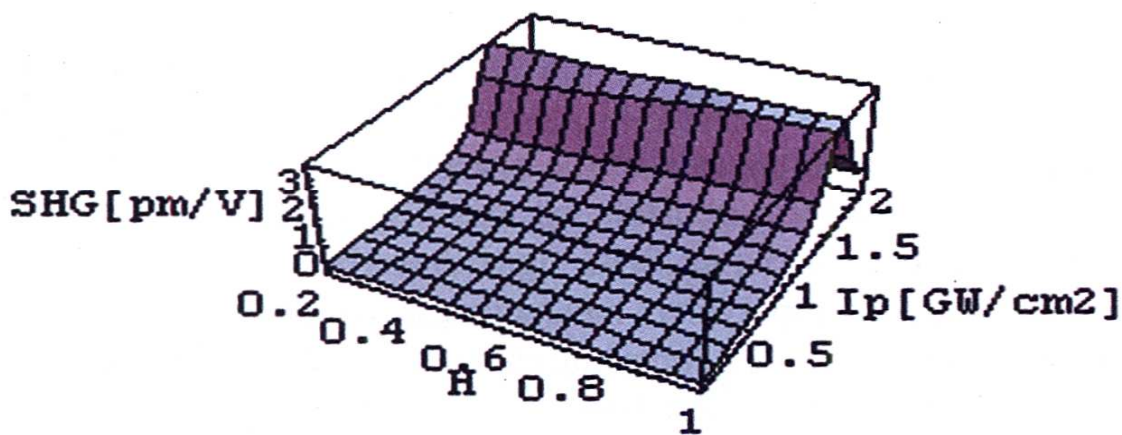
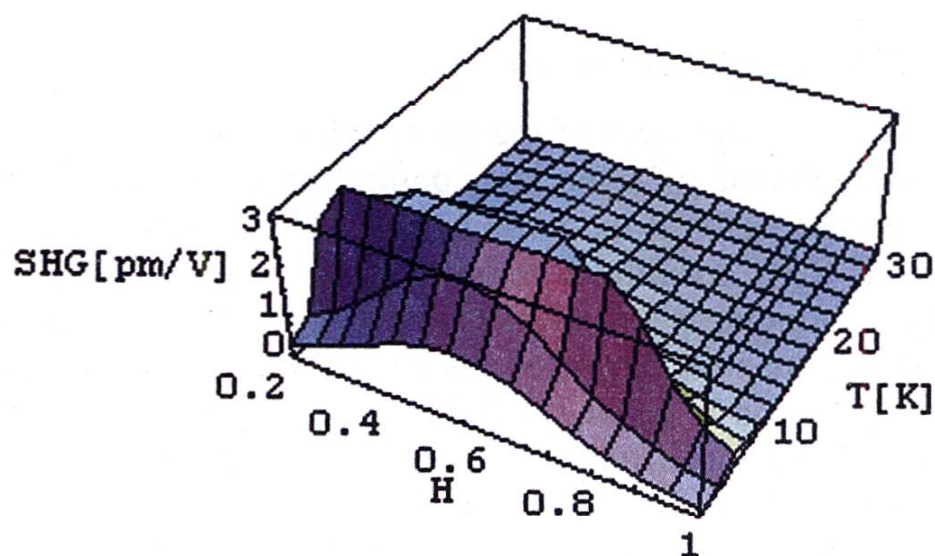


Fig. 2. Experimental dependence of the photoinduced SHG versus degree of hexagonality  $H$  and pumping intensity  $I_p$



**Fig. 3.** Dependence of the photoinduced SHG versus temperature and degree of hexagonality

Temperature measurements for the photoinducing SHG averaged within the  $1.4 - 2.1 \text{ GW/cm}^2$  light power are shown in the Fig. 3. One can see that decreasing temperature favors increasing SHG at low temperatures. Increasing hexagonality (contrary to the photoinducing dependences) shifts the temperature photoinduced SHG towards the lower temperature. The obtained behaviours reflect probably a competition between the long-range temperature reorientation and space interaction between the particular nanocrystallites due to the hexagonally-induced non-centrosymmetry.

In order to evaluate the role of the photopolymer olygoetheracryalte matrices the analogous measurements on the TiC nanocrystallite films have shown that the maximal output SHG signal have been fiveth times less. The olygoetheracrylate photopolymers have also the vanishing values of the SHG [17–19]. Therefore the main contribution to the nonlinear optical susceptibility in this case belongs to guest-host interfaces. Theoretical simulations concerning the contributions of the particular fragments of the composites will be presented in a separate work.

## Conclusions

The new composite materials consisting of the TiC nanocrystallites embedded within the photopolymer olygoetheracryalte matrices are proposed.



The maximum photoinduced SHG is achieved for the hexagonality degree about 0.95 and is equal about  $10.1 \pm 0.13$  pm/V for the  $\chi_{222}$  tensor components. The optimal concentration necessary to achieve the maximal SHG signal of the embedded TiC nanopowders lies within the 0.8 – 1.6% for the time delay between the photoinducing UV nitrogen laser signal and probe YAG:Nd probing signal about 20 ps. Decreasing temperature stimulates an increase of the output photoinduced SHG signal. The analogous measurements on the TiC nanocrystallite films have shown that the maximal output SHG signal have been fiveths times less. Therefore the main contribution belongs to guest-host interfaces. The hexagonality is closely connected with the sizes of the nanocrystallites as well with the degree of the non-centrosymmetry defining the nonlinear optical susceptibility.

## References

- [1] C.R. Kagan, C.B. Murray, M. Nirmal, and M.G. Bawendi, *Phys. Rev. Lett.*, **76**, 1517 (1996).
- [2] A. Mews, A.V. Kadavanich, U. Banin, and A.P. Alivisatos, *Phys. Rev.*, **B53**, 13242 (1996).
- [3] D.J. Norris, and M.G. Bavendi, *J.Chem.Phys.*, **103**, 5260 (1995).
- [4] D.J. Norris, and M.G. Bavendi, *Phys. Rev.*, **B53**, 16338(1996).
- [5] N.A. Hill, and K.B. Whaley, *Phys. Rev.Lett.*, **75**, 1130 (1995).
- [6] R.W. Schoenlein, D.M. Mittelman, J.J. Shiang, A.P. Alivisatos, and C.V. Shank, *Phys.Rev. Lett.*, **70**, 1014 (1993).
- [7] Y. Li, M. Takata, and A. Nakamura, *Phys.Rev.*, **57B**, 9193 (1998).
- [8] „Nonlinear Optical Effects in Organic Polymers”, NATO ASI Series, Series E: Applied Sciences, V. 162, J. Messier, F. Kajzar, P. Prasad and D. Ulrich, eds (Kluwer Academic Publishers, Dordrecht, 1989).
- [9] „Materials for Nonlinear Optics”, American Chemical Society, ACS Symposium Series, V. 455, S.R. Marder, J.E. Sohn, and G.D. Stucky eds. (ACS, Washington, DC, 1991).
- [10] M. Kuzyk, C. Poga, in: „Molecular Nonlinear Optics”, 1994, Ch. 7, Academic Press, NY., 209.
- [11] I.V. Kityk, R.I. Mervinskii, J. Kasprczyk and S. Jossi, *Materials Letters*, **27**, 233 (1996).
- [12] C. Fiorini, F. Charra, J.M. Nunzi, P. Raymond, *Nonlinear optics*, 1994, V. 22, 16; I.V. Kityk, M. Matusiewicz, J. Ksperczyk, M. Piasecki, *Ferro-electrics*, , **191**, 147 (1997).

- [13] M.M. Cauchetier, O. Cloix and M. Luce, *Adv. Ceram. Mater.* 3,6 (1988) 548.
- [14] S. Charpentier Ph.D. thesis-Universite du Maine (1998).
- [15] S.N. Rachkeev, W.R.L. Lambrecht, B. Segall, *Phys.Rev.*, B57, 9705 (1998).
- [16] B. Sahraoui, I.V. Kityk, M. Czerwinski, J. Kasperczyk, *High Performance Polymers*, 9, 51 (1997).
- [17] M. Czerwinski, J. Bieleninik, J. Napieralski, I.V. Kityk, J. Kasperczyk, R.I. Merwinski, *Europ.Polymer Journ.*, 33, 1441 (1997).
- [18] M. Czerwinski, R.I. Merwinski, M. Kulesza, I.V. Kityk, J. Kasperczyk, *Materials Chemistry and Physics*, 205, 107 (1998).
- [19] R.I. Merwinski, I.V. Kityk, M. Makowska-Janusik, J. Straube, M. Matusiewicz, J. Kasperczyk, *Optical Materials*, 6, 239 (1996).
- [20] E.B. Nowikow. Problems of separation nanocrystallite by sizes. Preprint Inst. Nadtw.Materialow, AN USSR – 156, 1990, 65 p.

R. MERWINSKII and L. GUDZOWSKA

**TiC Nanocrystals Embedded in Oligoetheracrylate Photopolymer Matrices  
as New Promising Nonlinear Optical Materials**

**Summary**

Photoinduced optical phenomena in TiC nanocrystallites embedded within the photo-polymer oligoetheracrylate matrices have been studied using experimental nonlinear optics, particularly photoinduced optical second harmonic generation (SHG). The YAG-Nd-laser ( $\lambda = 1.06 \mu\text{m}$ ;  $W = 30 \text{ MW}$ ; pulse duration within the 30 – 50 ps) was used as a source of pumping light and the nitrogen laser ( $\lambda = 337 \text{ nm}$ ) have been applied as a source of the photoinducing light. With increasing intensity of the photoinducing beam, the SHG ( $\lambda = 0.53 \mu\text{m}$ ) signal increased and achieved a maximum ( $\chi_{222} = 10.1 \pm 0.13 \text{ pm/V}$ ) at a photon flux of about  $1.61 \text{ GW/cm}^2$ . With decreasing temperature, the SHG signal strongly increases within the temperature range 25 – 30 K. Time-dependent probe-pump measurements indicate an existence of the SHG maximum for a pump-probe time delay of about 20 ps. The TiC hexagonal structural components play a key role in the observed photoinduced nonlinear optical effects. Large values of the nonlinear optical constants as well the good technological parameters open a possibility to enhance the nonlinear optical susceptibilities.